Molecular Complexation as a Design Tool in the Crystal Engineering of Noncentrosymmetric Structures. Ideal Orientation of Chromophores Linked by O−H···O and C−H···O Hydrogen Bonds for Nonlinear Optics

Meiyappan Muthuraman,[†] René Masse,*[,†] Jean-François Nicoud,[‡] and Gautam R. Desiraju[§]

Laboratoire de Cristallographie associé à l'Université Joseph Fourier, CNRS, BP166, 38042 Grenoble-Cedex, France, Groupe des Matériaux Organiques, Institut de Physique et Chimie des Matériaux de Strasbourg, CNRS et Université Louis Pasteur (UMR 7504), 23 rue du Loess, 67037 Strasbourg Cedex, France, and School of Chemistry, University of Hyderabad, Hyderabad 500 046, India

Received November 22, 2000. Revised Manuscript Received January 23, 2001

Six molecular complexes formed between 4-hydroxy-4′-nitrobiphenyl/stilbene and a 4-substituted pyridine-1-oxide [methyl (**1**,**2**), cyano (**3**,**4**), and nitro (**5**,**6**)] have been studied with the specific aim of assessing a new design strategy for the molecular complexation of new materials that show quadratic nonlinear optical behavior. Five of them (**1**−**4** and **6**) exhibit second harmonic generation (SHG) activity when illuminated with 1064-nm Nd^{3+}:YAG laser light and, hence, crystallize in noncentrosymmetric space groups. The biphenyl/stilbene component forms a two-dimensional slab structure mediated by phenyl···phenyl (C···H and C···C) interactions, and the polar axes of the biphenyl/stilbene are in an antiparallel alignment. In complexes **1**−**5**, the pyridine-1-oxide component occupies the interslab spaces and is bound to the slabs with strong O−H···O and O−H···N and weak C−H···O hydrogen bonds. In complexes **1**−**4**, the pyridine-1-oxide component is arranged in a herringbone motif, with an optimal orientation thus contributing favorably to the bulk NLO efficiency. This efficiency is equivalent to that of 3-methyl-4-nitropyridine-1-oxide (POM). Complexes **1** and **2** have similar crystal structures in space group $P2_1$ and comparable lattice constants. Similarly, **3** and **4** have identical crystal packing patterns in space group $Pca2_1$. In **5** (space group $P2_1/a$), the 4-nitropyridine-1-oxide occupies the space between the slabs in the form of antiparallel dimers. In complex **6** (space group $P2_{1)}$, the slab structure is much changed, without any interslab spacing, and the 4-nitropyridine-1-oxide is also involved in slab formation. Crystals of **6** show a detectable SHG activity equivalent to that of urea.

Introduction

Organic nonlinear optical materials are of much interest to chemists, material scientists, and optical physicists because of their superior performance with respect to their nonlinear optical responses.[1] Organic materials offer various advantages over conventional inorganic NLO materials, including high optical nonlinearities, fast response times, facile modification of molecular properties through precise synthetic methods, and high optical damage thresholds.[2] However, the transfer of these materials into actual devices, and thus marketable products, is not straightforward, as stringent requirements such as noncentrosymmetric packing of NLO chromophores, low optical losses from either absorption or scattering, and environmental and photochemical stabilities have to be considered. Even if noncentrosymmetry were to be achieved, the NLO chromophores need to be packed with an ideal orientation in the crystals in order to attain a maximum efficiency with phase-matching conditions.[3] The engineering of this orientation is still very much a matter of chance rather than design.

Crystal engineering strategies, based on an understanding of interactions such as charge transfer, electrostatic, hydrogen bonding, van der Waals attractions, and $\pi-\pi$ stacking, have also attracted much recent interest.[4] One aims at particular patterns such as ribbons, sheets, or layers making use of the above understanding, leading to functionalized materials with optimized properties of interest (electron or photon conduction, ferromagnetic, or nonlinear optical) at a

* Author to whom correspondence should be addressed. E-mail: masse@labs.polycnrs-gre.fr.
[†] Laboratoire de Cristallographie associé à l'Université Joseph Fourier.
[‡] Institut de Physique et Chimie des Matériaux de Strasbourg.
[§] University of Hyderabad.

(1) Marder, S. R.; Sohn, J. E.; Stucky, G. D. *Materials for Nonlinear Optics*; ACS Symposium Series 445; American Chemical Society: Washington, D.C., 1991.
(2) *Nonlinear Optical Properties of Organic Molecules and Crystals*; Chemla, D. S., Zyss, J., Eds.; Academic Press: New York, 1987; Vols. 1 and 2.
(3) Zyss, J.; Oudar, J.-L. *Phys. Rev. A* **1982**, *26*, 2028.
(4) Desiraju, G. R. *Crystal Engineering: The Design of Organic Solids*; Elsevier: Amsterdam, 1989.

10.1021/cm000927y CCC: $20.00
Published on Web 04/10/2001

Scheme 1. (a) Pair of Chromophores (in the Complex) Formed by Strong, Linear O−H···O Interaction. (b) Two Possible Orientations of the Pair

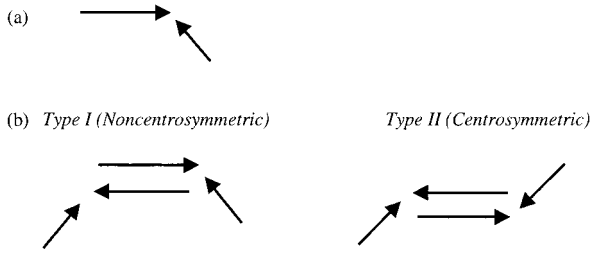

supramolecular level. In nonlinear optics, various approaches have been attempted to pack the organic chromophores in a noncentrosymmetric fashion and to thus optimize the bulk properties; these approaches include hydrogen bonding, chiral substitution, vanishing dipole moments, and inclusion compound formation.[5]

Pan et al. utilized the antiparallel packing of dipolar molecules to design an efficient electrooptic crystal.[6] They chose a merocyanine-based chromophore, the neutral zwitterionic and protonated forms of which have opposite signs of molecular hyperpolarizabilities (β), so that when their dipolar axes assume antiparallel packing, the molecular hyperpolarizabilities are added together. Another approach could be to design molecular complexes with two complementary polar molecules in such a way that, when one constituent goes into an antiparallel packing, the other is forced to pack with a polar alignment (Scheme 1). Usually, the more polar constituent tends to align in an antiparallel fashion, forcing the weaker constituent to adopt either a polar or apolar alignment, depending on the possibilities of other hydrogen-bonding interactions. The scope of this strategy is explored in this work. We selected three different 4-substituted pyridine-1-oxides and 4-hydroxy-4′-nitrobiphenyls/stilbenes as complementary NLO chromophores for cocrystallization. The selected biphenyl and stilbene derivatives are known to be good hyperpolarizable chromophores. Pyridine-1-oxides have already been investigated as NLO chromophores by using the so-called "push−pull" effect of the N-oxide bond in the intramolecular charge transfer at the origin of the hyperpolarizability.[5c,7] In these systems, the biphenyl/stilbene is expected to adopt an antiparallel packing. Also, aromatic hydrocarbons are known to utilize C···H and C···C interactions, which are isotropic in nature.[8] Such interactions would be expected to lead to a stable 2D slab structures in biphenyls and stilbenes, thus providing room for the pyridine-1-oxide molecules between the slabs. Finally, the O atom of the pyridine-1-oxide is a better hydrogen-bond acceptor and forms strong nearly linear O−H···O hydrogen bonds with protic hydrogen-bond donors.[9] This work is an early demonstration of the design strategy described above to achieve ideal orientation of one of the chromophores.

Experimental Section

Materials Synthesis. 4-Hydroxy-4′-nitrobiphenyl was prepared by literature methods.[10] 4-Hydroxy-4′-nitrostilbene, substituted pyridine-1-oxides, methanol, and acetonitrile were used as purchased without further purification. Complexes **1**−**6** were grown by slow evaporation from equimolar mixtures of the respective components in acetonitrile or methanol. In a typical experiment, 0.245 g of 4-hydroxy-4′-nitrobiphenyl (0.001 mol) and 0.109 g of 4-methylpyridine-1-oxide (0.001 mol) were dissolved separately in 10 mL of methanol. The two solutions above were mixed and stirred at 40 °C for 15 min and then filtered. Crystals of complex **1** appeared in a few days and were separated from solution before the solvent evaporated completely.

Complexes **1**−**5** are generally grow in bulky shapes as good-quality yellow crystals, whereas **6** grows as red dentritic needles with poor X-ray quality. The melting points of the compounds were measured using an Electrothermal 9100 digital melting point apparatus at a heating rate of 1 °C/min. Complexes **1** and **3** have similar melting points (154 and 152 °C, respectively), as do **2** and **4** (181° and 182 °C, respectively). The observed similarities in the melting points indicate that the crystal packing energies mostly arise from the packing of the biphenyl or stilbene partners, irrespective of the counter molecule in the complex (4-methyl or 4-cyanopyridine-1-oxide).

Second Harmonic Generation Powder Tests. The NLO efficiencies of complexes **1**−**6** were evaluated by the Kurtz and Perry[11] powder test. Noncalibrated freshly crystallized materials were used for the second harmonic generation experiments. The fundamental beam was emitted by a Q-switched, mode-locked Nd^{3+}:YAG laser operating at 1.06 μm and generating pulse trains at a 10-Hz repetition rate. The pulse duration was ~10 ns, and the fluence was 400 mJ/cm^2. The NLO efficiency was estimated by eye by comparison with the signals of crystalline POM and urea having the same average granulometry. SHG signals of complexes **1**−**4** are equivalent to that of POM. Signals of complex **6** could be compared to that of urea. Complex **5** is SHG-inactive.

X-ray Diffraction. The space groups and cell parameters of the complexes were determined using an Enraf-Nonius CCD diffractometer with Ag Kα radiation. Diffracted intensities were corrected for Lorentz and polarization factors. No absorption correction was applied because of a favorable crystal geometry and a low absorption coefficient in each case. The crystal data, details of the diffracted intensity measurements, and refinement conditions for crystals **1**−**6** are summarized in Table 1, and the asymmetric units are shown in Figure 1. The structures were solved by direct methods using the SIR 92 program.[12] Full-matrix least-squares refinements were performed on F with teXsan software.[13] Scattering factors for neutral atoms and f', $\Delta f'$, f'', and $\Delta f''$ were taken from the International Tables for X-ray Crystallography.[14] The crystal structures were drawn using the ORTEP program[15] included in teXsan software and the MolView program.[16] Selected interatomic distances and bond angles are listed in Tables 2

(5) (a) Muthuraman, M.; Le Fur, Y.; Bagieu-Beucher, M.; Masse, R.; Nicoud, J.-F.; Desiraju, G. R. *J. Mater. Chem.* **1999**, *9*, 2233. (b) Zyss, J.; Nicoud, J.-F.; Coquillay, M. *J. Chem. Phys.* **1984**, *81*, 4160. (c) Zyss, J.; Chemla, D. S.; Nicoud, J.-F. *J. Chem. Phys.* **1981**, *74*, 4800. (d) Ramamurthy, V.; Eaton, D. F. *Chem. Mater.* **1994**, *6*, 1128. (e) Eaton, D. F.; Anderson, A. G.; Tam, W.; Wang, Y. *J. Am. Chem. Soc.* **1987**, *109*, 1886. (f) König, O.; Hulliger, J. *Nonlinear Opt.* **1997**, *17*, 127.

(6) Pan, F.; Wong, M. S.; Gramlich, V.; Bosshard, C.; Günter, P. *J. Am. Chem. Soc.* **1996**, *118*, 6315.

(7) Pécaut, J.; Le Fur, Y.; Lévy, J. P.; Masse, R. *J. Mater. Chem.* **1993**, *3*, 333.

(8) (a) Williams, D. E. *Acta Crystallogr.* **1974**, *A30*, 71. (b) Williams, D. E. *Acta Crystallogr.* **1980**, *A36*, 715. (c) Desiraju, G. R.; Gavezotti, A. *J. Chem. Soc., Chem. Commun.* **1989**, 621. (d) Gavezotti, A. *Chem. Phys. Lett.* **1989**, *161*, 67.

(9) (a) Albini, A.; Pietra, S. *Heterocyclic N-Oxides*; CRC Press: Boca Raton, FL, 1991. (b) Nelson, J. H.; Nathan, L. C.; Ragsdale, R. O. *J. Am. Chem. Soc.* **1968**, *90*, 5754.

(10) Jones, B.; Chapman, F. *J. Chem. Soc.* **1952**, 1929.

(11) Kurtz, S. K.; Perry, T. T. *J. Appl. Phys.* **1968**, *39*, 3798.

(12) Altomare, A.; Cascarano, M.; Giacovazzo, C.; Guagliardi, A. J. *Appl. Cryst.* **1993**, *26*, 343.

(13) Molecular Structure Corporation. *teXsan for Windows, Single-Crystal Structure Analysis Software*, versions 1.03 and 1.04; Molecular Structure Corporation: The Woodlands, TX, 1997−1998.

Table 1. Crystallographic Data of Complexes 1−6

	1	2	3	4	5	6
formula	$C_6H_7NO-C_{12}H_9NO_3$	$C_6H_7NO-C_{14}H_{11}NO_3$	$C_6H_4N_2O-C_{12}H_9NO_3$	$C_6H_4N_2O-C_{14}H_{11}NO_3$	$C_5H_4N_2O_3-C_{12}H_9NO_3$	$C_5H_4N_2O_3-C_{14}H_{11}NO_3$
FW	324.34	350.37	335.32	361.36	355.31	381.34
crystal sys.	monoclinic	monoclinic	orthorhombic	orthorhombic	monoclinic	monoclinic
space group	$P2_1$ (4)	$P2_1$ (4)	$Pca2_1$ (29)	$Pca2_1$ (29)	$P2_1/a$ (14)	$P2_1$ (4)
a (Å)	5.6171(5)	5.3737(8)	37.170(3)	41.576(3)	14.0195(5)	12.305(2)
b (Å)	7.7555(1)	7.9572(1)	5.6947(4)	5.4115(2)	8.1263(4)	5.6420(7)
c (Å)	18.185(2)	20.561(4)	7.6038(6)	7.8364(6)	15.0153(6)	25.979(4)
α/°	90	90	90	90	90	90
β/°	94.719(10)	97.938(10)	90	90	108.207(2)	103.401(5)
γ/°	90	90	90	90	90	90
Z	2	2	4	4	4	4
V (Å^3)	789.52(9)	870.7(2)	1609.5(2)	1763.1(2)	1625.0(1)	1754.5(4)
D_{calc} (Mg m^{-3})	1.364	1.336	1.384	1.361	1.452	1.444
R (R_w)	4.95 (4.56)	4.88 (4.80)	4.22 (3.93)	3.35 (2.70)	4.25 (4.80)	6.11 (6.40)
total refl.	1720	4377	1598	1244	2315	2603
unique refl.	1387 (I>2σ(I))	1881 (I>2σ(I))	1180 (I>1σ(I))	1072 (I>1σ(I))	1748 (I>3σ(I))	1488 (I>3σ(I))
parameters	216	234	225	243	235	504
crystal shape and color	prism, yellow	prism, yellow	prism, yellow	prism, yellow	prism, yellow	dentritic needle, red
solvent	CH_3CN	CH_3CN	MeOH	MeOH	MeOH	MeOH/ CH_3CN
diffract	CCD	CCD	CCD	CCD	CCD	CCD
SHG	POM	POM	POM	POM	0	urea
mp (°C)	154	182	152	181	140	141

and 3. Final atomic parameters, anisotropic thermal factors, and isotropic thermal factors for H atoms and a list of observed and calculated structure factors are available as deposit materials.

Results and Discussion

Complexes 1 and 2. Complexes **1** and **2**, both SHG-active with a signal equivalent to that of POM at 1.06 μm, crystallize in the same space group, $P2_1$, and have similar unit cell parameters (Table 1). The extension of conjugation through the introduction of the CH═CH group in **2** does not alter the packing pattern or the space group, except for an increase in the c parameter. No proton transfer is observed between phenyl OH and N-oxide groups. However, there are strong O−H···O and O−H···N hydrogen bonds (Tables 2 and 3) that hold the component molecules together. The two phenyl rings of the biphenyl and stilbene component are nearly coplanar (∼1° out of plane for biphenyl and ∼2° for stilbene), indicating effective conjugation between the two phenyl rings. However, these efficient NLO chromophores (4-hydroxy-4′-nitrobiphenyl and 4-hydroxy-4′-nitrostilbene) align with their polar axes antiparallel and with their planes nearly perpendicular (interplanar angles between adjacent biphenyl/stilbene are ∼66° for **1** and ∼75.0° for **2**), forming a zigzag tape running along [010]. The adjacent tapes are held together with C···C and C···H interactions, and the overall result is a 2D slab structure in the (110) plane (Figure 2).

Polynuclear aromatic entities are known to crystallize in one of four basic structure types: herringbone, γ, β, and sandwich-herringbone, and the major motifs in these four prototypes are the stack or layer and the glide or herringbone.[17] Gavezzotti and Desiraju analyzed the crystal packing of various polynuclear aromatic hydrocarbons and predicted that these structure types contain C···C, C···H, or H···H interactions that direct the packing pattern to one of these types.[18] The C···H interactions in these structures have been more lately referred to as being of the C−H···π type. In complex **1**, there is a weak C−H···π (Ph) (C···π = 3.757 Å) interaction in addition to the Ph···Ph interactions (C···H) between the biphenyl molecules in the tape.[19] Also, the activated C−H group ortho to the NO_2 group is involved in a C−H···O (C···O = 3.617 Å) interaction with the phenyl O atom. In **2**, the C−H···π (Ph) interactions are much weaker, and a similar slab structure is formed but with Ph···Ph interactions. In addition, the π electrons of the CH═CH group act as a hydrogen-bond acceptor, forming weak C−H···π interactions within the tape, as well as between tapes (C···π = 3.561 and 3.735 Å). A view down the molecular axis [001] reveals that the Ph···Ph interactions (C···H) involve four biphenyl/stilbene molecules forming a square-shaped motif (Figure 2). These interactions extend in two dimensions to form a herringbone structure such as is seen in benzene, terphenyl, quaterphenyl, and 2-aminophenol. The Ph···Ph interactions are highly stabilizing in nature, and Dance et al. have analyzed various kinds of Ph···Ph interactions, the so-called tetraphenyl and hexaphenyl embraces, as dominant motifs in a series of compounds containing tetraarylphosphonium cations.[20]

The smaller NLO chromophore 4-methylpyridine-1-oxide occupies the interslab spacing, oriented in the same direction in both complexes **1** and **2** (Figure 3). These chromophores form a herringbone pattern in themselves and are bound to the slabs through O−H···O and O−H···N hydrogen bonds on one side and through C−H···O interactions on the other, thus joining the adjacent slabs along the [001] direction. The biphenyl/stilbene moieties are offset alternately in the 1D

(14) *International Tables for Crystallography*; Wilson, A. J. C., Ed.; Kluwer Academic Publishers: Dordrecht, The Netherlands, 1992; Vol. C, Tables 4268, 6111, and 6112.
(15) Johnson, C. K. *ORTEP II*; Report ORNL-5138; Oak Ridge National Laboratory: Oak Ridge: TN, 1976.
(16) Cense, J.-M. MolView, Molecular Graphics for the Macintosh. In *Modelling of Molecular Structures and Properties*; Elsevier: Amsterdam, 1990; pp 763−766.
(17) Desiraju, G. R.; Gavezotti, A. *Acta Crystallogr.* **1989**, *B45*, 473.
(18) Gavezzotti, A.; Desiraju, G. R. *Acta Crystallogr.* **1988**, *B44*, 427.
(19) Desiraju, G. R.; Steiner, T. *The Weak Hydrogen Bond in Structural Chemistry and Biology*; Oxford University Press: New York, 1999.
(20) Scudder, M.; Dance, I. *J. Chem. Soc., Dalton Trans.* **1998**, 3155.

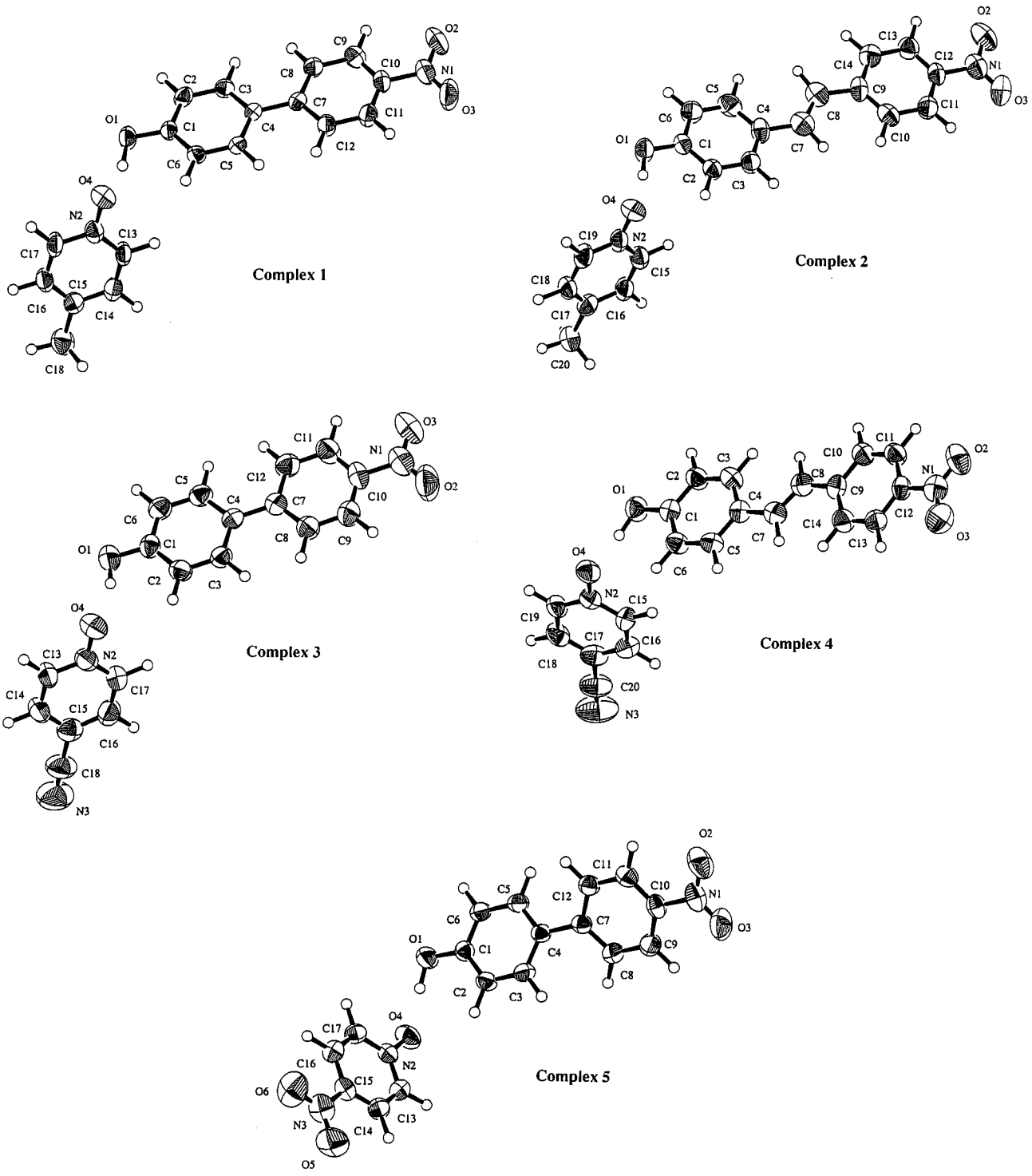

Figure 1. Crystallographic asymmetric units in structures **1**−**5**.

tape and thus provide exact room for the pyridine-1-oxides (Figure 3). The polar axis (O → CH_3) of the 4-methylpyridine-1-oxide makes an angle of 57.4° and 57.5° (respectively, for **1** and **2**) with [010]. These angles are very close to the optimal angle (54.74°) for an efficient contribution of molecular polarizability to the bulk NLO property in the point group 2.[3] Such a quasi-ideal orientation of 4-methylpyridine-1-oxide chromophores explains an NLO efficiency equivalent to that of POM.

Complexes 3 and 4. Complexes **3** and **4**, both SHG-active and with signals equivalent to that of POM at 1.06 μm, crystallize in the space group $Pca2_1$ and have comparable lattice constants. The packing pattern is very similar to those of **1** and **2** (Figure 3). There is no proton transfer between OH and N-oxide, and the biphenyls/stilbenes form a 2D slab structure in the (011) plane mediated by C−H···π (Ph) interactions. In addition, the π electrons of the CH=CH moiety are also involved in hydrogen bonding in **4** (Table 3). The 4-cyanopyridine-1-oxide occupies the interslab spacing with a herringbone motif (similar to **1** and **2**) and is held by O−H···O and O−H···N hydrogen bonds on one side and by C−H···O and C−H···N hydrogen bonds on the

Table 2. Selected Interatomic Distances (Å) and Angles (°) for Complexes 1−5[a]

Complex **1**				Complex **4**			
C1−O1	1.372(3)	C1−O1−H1	106.3	C1−O1	1.361(3)	C1−O1−H1	109.2
O1−H1	1.13	O4−N2−C13	120.9(3)	O1−H1	1.04	O4−N2−C15	119.7(3)
C10−N1	1.459(4)	O4−N2−C17	118.7(3)	C12−N1	1.467(5)	O4−N2−C19	118.5(2)
N1−O2	1.232(4)	C13−N2−C17	120.4(3)	N1−O2	1.216(4)	C15−N2−C19	121.8(3)
N1−O3	1.218(4)			N1−O3	1.233(3)		
N2−O4	1.333(4)			N2−O4	1.318(3)		
Complex **2**				Complex **5**			
C1−O1	1.367(3)	C1−O1−H1	108.3	C1−O1	1.362(2)	C1−O1−H1	110.3
O1−H1	1.08	O4−N2−C15	121.1(3)	O1−H1	1.02	O4−N2−C13	119.6(2)
C12−N1	1.445(4)	O4−N2−C19	119.7(3)	C10−N1	1.465(3)	O4−N2−C17	119.6(2)
N1−O2	1.214(4)	C15−N2−C19	119.2(3)	N1−O2	1.214(3)	C13−N2−C17	120.8(2)
N1−O3	1.235(4)			N1−O3	1.219(3)		
N2−O4	1.325(4)			N2−O4	1.311(2)		
Complex **3**							
C1−O1	1.368(3)	C1−O1−H1	102				
O1−H1	0.94	O4−N2−C13	117.6(3)				
C10−N1	1.468(5)	O4−N2−C17	120.4(3)				
N1−O2	1.231(4)	C13−N2−C17	122.0(3)				
N1−O3	1.218(4)						
N2−O4	1.323(3)						

[a] Estimated standard deviations are given in parentheses.

Table 3. Hydrogen Bonding Interactions in Complexes 1−5

D−H···A	H···A (Å)	D···A (Å)	D−H···A (°)	D−H···A	H···A (Å)	D···A (Å)	D−H···A (°)
complex **1**				complex **3** (cont)			
O1−H1···O4	1.456(3)	2.562(3)	162.8	C16−H12···O2	2.623(4)	3.613(5)	152.3
O1−H1···N2	2.331(3)	3.335(5)	140.4	C17−H13···O1	2.368(2)	3.149(4)	128.0
C6−H5···O4	2.754(2)	3.428(4)	120.7	C2−H2···π(Ph)	3.053	3.920	138.2
C11−H8···O1	2.755(1)	2.617(4)	137.0	C8−H6···π(Ph)	2.848	3.712	137.6
C13−H10···O1	2.400(2)	3.143(4)	125.0	complex **4**			
C14−H11···O1	2.798(2)	3.333(4)	110.5	O1−H1···O4	1.589(2)	2.624(3)	173.1
C14−H11···O3	2.748(4)	3.702(5)	147.6	O1−H1···N2	2.452(3)	3.402(3)	151.6
C16−H12···O2	2.662(3)	3.673(4)	155.9	C6−H5···O4	2.654(2)	3.362(4)	123.5
C16−H12···O3	2.894(3)	3.869(4)	150.5	C10−H8···O1	2.822(3)	3.550(4)	125.1
C18−H15···O2	2.600(3)	3.488(5)	138.6	C10−H8···O4	2.744(2)	3.487(4)	126.2
C12−H9···π(Ph)	2.886	3.757	138.3	C11−H9···O4	2.832(2)	3.521(3)	121.7
complex **2**				C13−H10···O1	2.670(1)	3.609(3)	145.7
O1−H1···O4	1.518(3)	2.586(4)	169.6	C15−H12···O1	2.415(2)	3.221(4)	130.9
O1−H1···N2	2.391(3)	3.310(4)	142.2	C16−H13···O3	2.405(3)	3.417(4)	156.4
C2−H2···O4	2.649(2)	3.365(4)	123.7	C18−H14···O2	2.562(3)	3.573(5)	156.0
C11−H9···O1	2.724(1)	3.676(4)	144.5	C19−H15···N3	2.188(4)	3.146(5)	147.7
C13−H11···O4	2.692(3)	3.453(5)	125.4	C2−H2···π(CH=CH)	2.749	3.683	145.5
C14−H12···O1	2.809(3)	3.557(4)	124.0	C6−H5···π(Ph)	3.035	3.938	142.8
C14−H12···O4	2.809(3)	3.504(5)	119.9	complex **5**			
C15−H13···O1	2.420(2)	3.193(4)	125.9	O1−H1···O4	1.627(1)	2.650(2)	174.7
C16−H14···O3	2.526(4)	3.542(5)	150.5	O1−H1···N2	2.527(2)	3.497(2)	157.5
C18−H16···O2	2.567(3)	3.610(5)	158.1	C2−H2···O4	2.655(2)	3.366(3)	123.3
C20−H19···O2	2.647(3)	3.535(5)	136.7	C2−H2···O6	2.578(2)	3.410(3)	133.7
C3−H3···π(CH=CH)	2.768	3.735	144.7	C5−H4···O3	2.780(2)	3.568(3)	130.4
C6−H5···π(CH=CH)	2.816	3.561	125.0	C6−H5···O2	2.660(2)	3.700(3)	163.0
complex **3**				C6−H5···N1	2.697(2)	3.583(3)	139.6
O1−H1···O4	1.683(3)	2.588(3)	159.6	C12−H9···O3	2.737(2)	3.297(3)	118.8
O1−H1···N2	2.602(3)	3.421(4)	145.5	C13−H10···O4	2.321(2)	3.194(3)	136.8
C2−H2···O4	2.718(2)	3.412(4)	122.0	C13−H10···O6	2.869(2)	3.455(3)	114.3
C9−H7···O1	2.710(1)	3.560(4)	135.7	C14−H11···O1	2.576(2)	3.348(3)	128.1
C13−H10···N3	2.184(5)	3.183(5)	153.9	C17−H13···O5	2.580(2)	3.599(3)	158.0
C14−H11···O3	2.590(3)	3.583(4)	153.0	C9−H7···π(Ph)	2.925	3.745	133.6

other side of the slab. In addition, the 4-cyanopyridine-1-oxides are connected to each other with C−H···N hydrogen bonds. The polar axes (O → CN) of the pyridine-1-oxide chromophore in **3** and **4** make the ideal angles 53.3° and 54.7° (respectively, for **3** and **4**) with respect to [010]. Thus, the molecular polarizabilities of the weaker chromophores in **3** and **4** contribute to the bulk NLO property to almost the extent that is theoretically possible.

Complexes 5 and 6. Complexes **5** and **6** are built with the most hyperpolarizable pyridine-1-oxide chromophore used in this study. Unfortunately, poor NLO efficiencies are obtained, as **5** is SHG-inactive and **6** exhibits a SHG signal equivalent to that of urea. Complex **5** crystallizes in the centrosymmetric space group $P2_1/a$ and retains the slab structure in the (110) plane. However, this structure is offset along [001] (Figure 4). The two phenyl rings of 4-hydroxy-4′-nitrobiphenyl are out of plane by 32.4°, and hence, there is reduced conjugation between them. They form 1D tapes with C···H interactions approximately along [100]. The polar axes of the biphenyls are aligned parallel within the tape, and there is slight slippage so that the first phenyl ring of one biphenyl interacts with the second phenyl ring of the adjacent biphenyl. These tapes are connected via C···H interactions along [010] with their

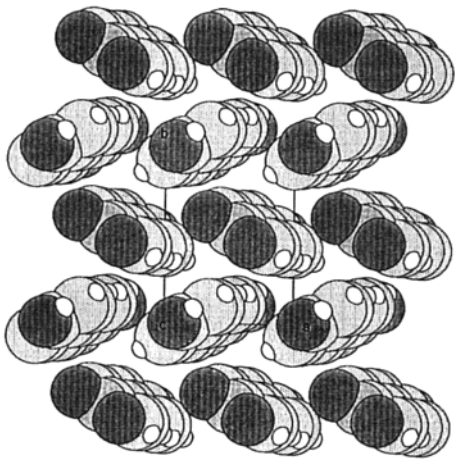

Figure 2. Two-dimensional slab structure in the (110) plane of 4-hydroxy-4′-nitrobiphenyl in complex **1**.

polar axes antiparallel, thus forming a 2D slab structure in the (110) plane. Viewed along the [001] axis, the slabs consist of biphenyl dimers arranged in a sandwich-herringbone fashion. The smaller NLO chromophore 4-nitropyridine-1-oxide occupies the interslab spacing in antiparallel pairs. In this centrosymmetric structure, both the biphenyl and N-oxide chromophores adopt antiparallel packing. The interaction of the biphenyl OH with the N-oxide is weak [O···O = 2.650(2) Å] compared with that in **1** and **3** [2.562(3) and 2.588(3) Å, respectively], indicating that the O atom of the 4-nitropyridine-1-oxide is not a very efficient hydrogen-bond acceptor. This could be due to the effective electron-withdrawing group in the para position. Between **1** and **3**, **1** has the shortest O···O distance, possibly because of the electron-donating nature of the methyl group compared to the weakly electron-withdrawing nature of the cyano group. Perhaps the weakening of the hydrogen bond between the constituents of complex **5** leads to an overall centrosymmetric packing.

The structure of **6** could not be solved properly, as the crystallization gives poor-quality dentritic crystals. However, the essential structural features were revealed in an approximate solution. Red crystals (space group $P2_1$) showed SHG activity close to that of urea. The phenolic hydrogen could not be found by difference Fourier syntheses because of insufficient diffraction data. Unlike the other complexes (**1**−**5**), which contain a pair of molecules (one molecule each of biphenyl/stilbene and pyridine-1-oxide) in the asymmetric unit, **6** contains two pairs of molecules (two molecules each of stilbene and pyridine-1-oxide). The 4-nitropyridine-1-oxide is also involved in slab formation and there is no interslab spacing (Figure 4). The slabs are connected

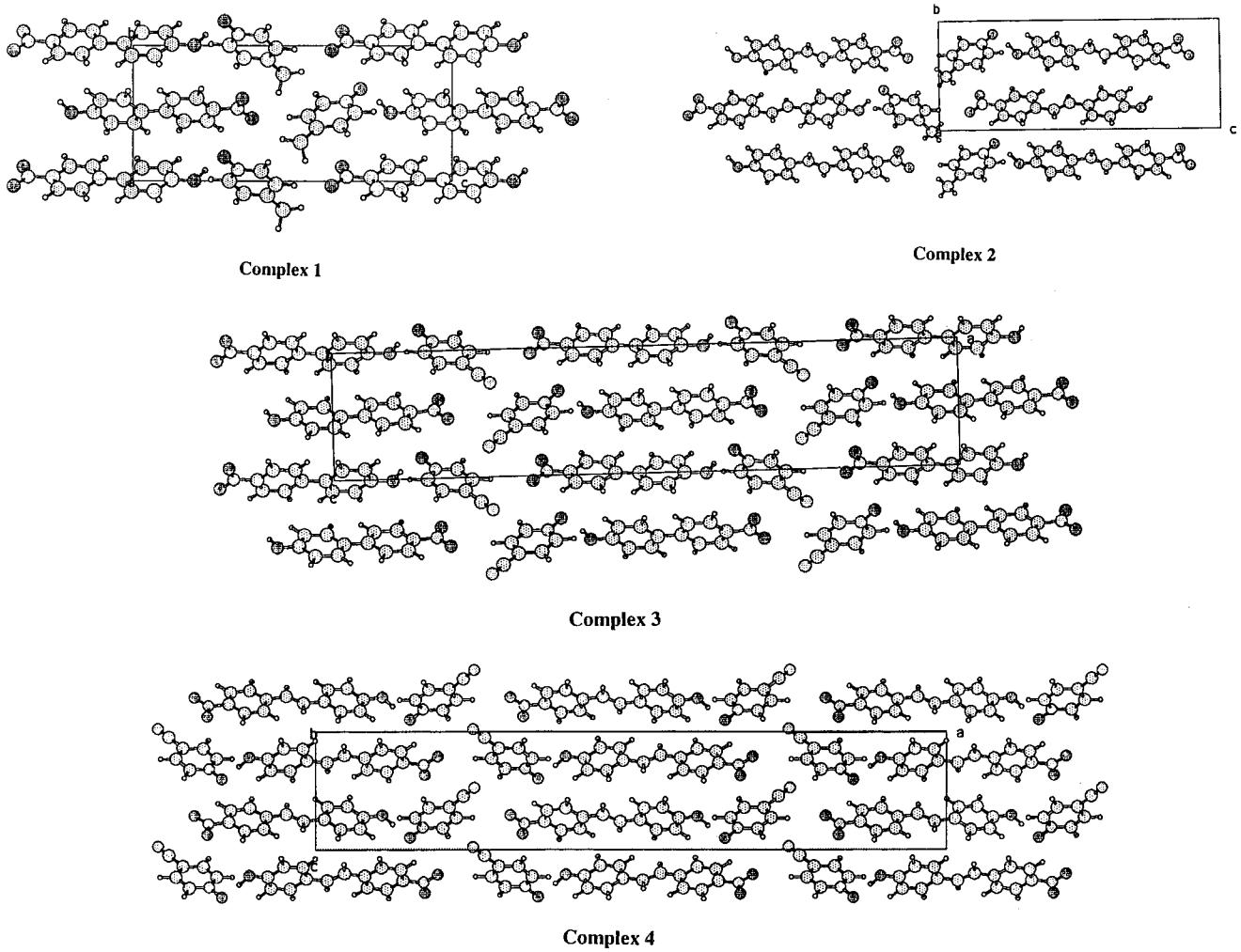

Figure 3. Quasi-ideal herringbone orientation of 4-methylpyridine-1-oxide in complexes **1** and **2** and of 4-cyanopyridine-1-oxide in complexes **3** and **4**.

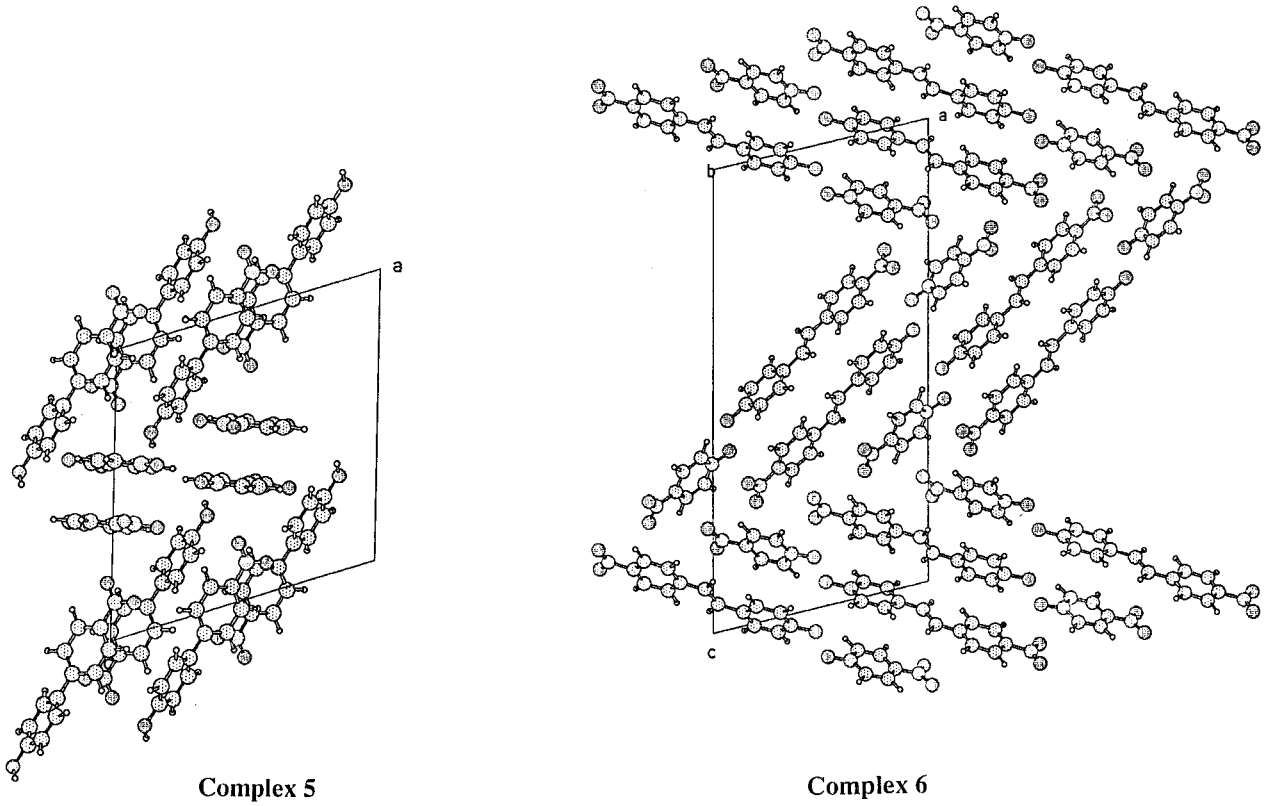

Figure 4. (Left) Crystal packing of complex **5** viewed in the (101) plane. (Right) Herringbone motifs of chromophores in complex **6**.

through C−H···O hydrogen bonds. Within the slab, the molecules are arranged in a herringbone motif.

Conclusions

The association of two chromophores in the same crystal opens up a new route to enhancing the probability of obtaining noncentrosymmetric structures and, with them, novel NLO materials. This approach is similar to the host−guest route wherein the stronger chromophore acts as the host and the weaker chromophore occupies the interslab spacing as the guest. Hulliger et al. explored a related method by incorporating NLO chromophores with a polar orientation in channels created with perhydrotriphenylene molecules.[21] In the present strategy, the dipolar interaction of the stronger counterpart is utilized to direct the weaker one to take up the ideal orientation. However, the selection of the chromophores is crucial because the size of the constitutent chromophores and the proper positioning of the potential hydrogen-bonding groups also have to be considered. The stronger chromophore always adopts an antiparallel packing, forcing the weaker one to assume a polar packing. From the structures of compounds **1**−**4**, it can be observed that, when the biphenyl/stilbene groups are translated alternately, the correct space is provided for the N-oxides to take up the polar orientation (Scheme 2). It is also seen that the weak C−H···O and C−H···N hydrogen bonds play a major role in these crystal structures. From a crystal engineering viewpoint, the strategy outlined in this paper is attractive because it resulted in the desired structural attribute in five cases out of six. Levels of robustness are high, and the stage seems to be set for electronic

Scheme 2

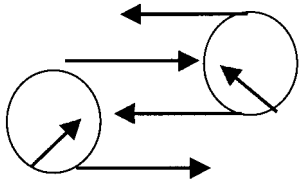

fine-tuning of the NLO components. However, a drawback appears in this strategy: the transparency of the crystals is presently limited by the most colored chromophore (biphenyl/stilbene), which does not contribute to the nonlinear macroscopic efficiency. Thus, the compromise between transparency and efficiency of such crystals might not be as good as that observed in crystals formed from two well-oriented chromophores of equivalent transparency, say, 4-pyridinone-4-nitrophenol.[22]

Acknowledgment. Financial support from the Indo-French Centre for the Promotion of Advanced Research, New Delhi, (IFCPAR Contract 1708-1) is gratefully acknowledged.

Supporting Information Available: Final atomic parameters, anisotropic thermal factors, and isotropic thermal factors for H atoms and a list of observed and calculated structure factors for crystals **1**−**6** (CIF). This material is available free of charge via the Internet at http://pubs.acs.org.

CM000927Y

(21) Hulliger, J.; König, O.; Hoss, R. *Adv. Mater.* **1995**, *7*, 719. König, O.; Bürgi, H−B.; Armbruster, T.; Hulliger, J.; Weber, T. *J. Am. Chem. Soc.* **1997**, *119*, 10632.

(22) Evans, C. C.; Bagieu-Beucher, M.; Masse, R.; Nicoud, J. F. *Chem. Mater.* **1998**, *10*, 847.